

The accelerating universe data of the high-redshift type Ia supernovae is consistent with a finite bounded expanding white hole universe without dark matter

John G. Hartnett*

School of Physics, the University of Western Australia

35 Stirling Hwy, Crawley 6009 WA Australia

(Dated: January 26, 2020)

Abstract

The distance modulus and supernova redshift data, determined by the high-z type Ia supernovae teams, is found to describe a model of the universe that is consistent with the Galaxy at the center of a finite spherically symmetric isotropic gravitational field. The result describes particles moving in both a central potential and an accelerating universe without the need for the inclusion of dark matter. That is, a finite bounded white hole with a radius $\Delta \geq 2 c\tau$. Using Carmeli's Cosmological General Relativity, the data cannot distinguish between the finite bounded model and the unbounded model described elsewhere. However the finite bounded model cannot be ruled out by the observations.

PACS numbers: 95.30.Sf 95.35.+d 98.62.Py 98.80.Es

*Electronic address: john@physics.uwa.edu.au

I. INTRODUCTION

In an interview with Scientific American George Ellis once said [10]

“People need to be aware that there is a range of models that could explain the observations, . . . For instance, I can construct you a spherically symmetrical universe with Earth at its center, and you cannot disprove it based on observations. . . . You can only exclude it on philosophical grounds. In my view there is absolutely nothing wrong in that. What I want to bring into the open is the fact that we are using philosophical criteria in choosing our models. A lot of cosmology tries to hide that.”

This paper proposes a model where the Galaxy is at the center of a spherically symmetric finite bounded universe. It contends that fits to the magnitude-redshift data, from the high- z type Ia supernovae (SNe Ia) teams, are also consistent with this model. This is providing that the radius of the Universe (a spherically symmetric matter distribution) is at least $2 c\tau$ where c is the speed of light and $\tau \approx 4.28 \times 10^{17}$ s (or 13.58 *Gyr*). Here τ is the Hubble-Carmeli time constant, or the inverse of the Hubble constant evaluated in the limits of zero gravity and zero distance.

This model is based on the Cosmological General Relativity (CGR) theory of Moshe Carmeli [4] but explores the motion of particles in a central potential. In this case the central potential is the result of the Galaxy being situated at the center of a spherical distribution comprising all matter in the Universe. This creates a unique point at the center toward which there is a net gravitational force on the Universe as a whole.

This paper is preceded by another paper [12], which will be called Paper I, that forms the basis of the work presented here. That paper described fits to the same data analyzed here but it assumed the unbounded model. The reader should be familiar with that paper before reading this.

A. Cosmological General Relativity

The metric [1, 2, 4] used by Carmeli (in CGR) in a generally covariant theory extends the number of dimensions of the Universe by the addition of a new dimension – the radial velocity of the galaxies in the Hubble flow. The Hubble law is assumed as a fundamental axiom for the Universe and the galaxies are distributed accordingly. The underlying mechanism is that

the substance of which space is built, the vacuum, is uniformly expanding in all directions and galaxies, as tracers, are fixed to space and therefore the redshifts of distant first ranked galaxies quantify the speed of the expansion.

In determining the large scale structure of the Universe the usual time dimension is neglected as observations are taken over such a short time period compared to the motion of the galaxies in the expansion. It is like taking a still snap shot of the Universe and therefore only four co-moving co-ordinates $x^\mu = (x^0, x^1, x^2, x^3) = (\tau v, r, \theta, \phi)$ are used – three of space and one of velocity. The parameter τ , the Hubble-Carmeli constant, is a universal constant for all observers.

Here the CGR theory is considered using a Riemannian four-dimensional presentation of gravitation in which the coordinates are those of Hubble, i.e. distance and velocity. This results in a phase space equation where the observables are redshift and distance. The latter may be determined from the high-redshift type Ia supernovae observations.

B. Phase space equation

The line element in CGR [5]

$$ds^2 = \tau^2 dv^2 - e^\xi dr^2 - R^2(d\theta^2 + \sin^2\theta d\phi^2), \quad (1)$$

represents a spherically symmetric isotropic universe, that is not necessarily homogeneous. The expansion is observed at a definite time and therefore $dt = 0$.

It is fundamental to the theory that $ds = 0$. In the case of Cosmological Special Relativity (see chap.2 of [4]), which is very useful pedagogically, we can write the line element as

$$ds^2 = \tau^2 dv^2 - dr^2, \quad (2)$$

ignoring θ and ϕ co-ordinates for the moment. By equating $ds = 0$ it follows from (2) that $\tau dv = dr$ assuming the positive sign for an expanding universe. This is then the Hubble law in the small v limit. Hence, in general, this theory requires that $ds = 0$.

Using spherical coordinates (r, θ, ϕ) and the isotropy condition $d\theta = d\phi = 0$ in (1) then dr represents the radial co-ordinate distance to the source and it follows from (1) that

$$\tau^2 dv^2 - e^\xi dr^2 = 0, \quad (3)$$

where ξ is a function of v and r alone. This results in

$$\frac{dr}{dv} = \tau e^{-\xi/2}, \quad (4)$$

where the positive sign has been chosen for an expanding universe.

II. SOLUTION IN CENTRAL POTENTIAL

Carmeli found a solution to his field equations, modified from Einstein's, (see Paper I [12] and [1, 4, 5]) which is of the form

$$e^\xi = \frac{R'}{1 + f(r)} \quad (5)$$

with $R' = 1$, which must be positive. From the field equations and (5) we get a differential equation

$$f' + \frac{f}{r} = -\kappa\tau^2\rho_{eff}r, \quad (6)$$

where $f(r)$ is function of r and satisfies the condition $f(r) + 1 > 0$. The prime is the derivative with respect to r . Here $\kappa = 8\pi G/c^2\tau^2$ and $\rho_{eff} = \rho - \rho_c$ where ρ is the averaged matter density of the Universe and $\rho_c = 3/8\pi G\tau^2$ is the critical density.

The solution of (6), $f(r)$, is the sum of the solution $(2GM/c^2r)$ to the homogeneous equation and a particular solution $(-\frac{\kappa}{3}\tau^2\rho_{eff}r^2)$ to the inhomogeneous equation. In [4] Carmeli discarded the homogeneous solution saying it was not relevant to the Universe, but the solution of a particle at the origin of coordinates, or in other words, in a central potential.

Now suppose we model the Universe as a ball of dust of radius Δ with us, the observer, at the center of that ball. In this case the gravitational potential written in spherical coordinates that satisfies Poisson's equation in the Newtonian approximation is

$$\Phi(r) = -\frac{GM}{r} \quad (7)$$

for the vacuum solution, but inside an isotropic matter distribution

$$\begin{aligned} \Phi(r) &= -G \left(\frac{4\pi\rho}{r} \int_0^r r'^2 dr' + 4\pi\rho \int_r^\Delta r' dr' \right) \\ &= \frac{2}{3}G\pi\rho r^2 - 2G\pi\rho\Delta^2, \end{aligned} \quad (8)$$

where it is assumed the matter density ρ is uniform throughout the Universe. At the origin ($r = 0$) $\Phi(0) = -2G\pi\rho_m\Delta^2$, where $\rho = \rho_m$ the matter density at the present epoch. In

general ρ depends on epoch. Because we are considering no time development ρ is only a function of redshift z and ρ_m can be considered constant.

From (8) it is clear to see that by considering a finite distribution of matter of radial extent Δ , it has the effect of adding a constant to $f(r)$ that is consistent with the constant $2G\pi\rho\Delta^2$ in (8), where $f(r)$ is now identified with $-4\Phi/c^2$.

Equation (5) is essentially Carmeli's equation A.19, the solution to his equation A.17 from p.122 of [4]. More generally (5) can be written as

$$e^\xi = \frac{R'^2}{1 + f(r) - K}, \quad (9)$$

where K is a constant. This is the most general form of the solution of Carmeli's equation A.17. So by substituting (9) into Carmeli's A.18, A.21 becomes instead

$$\frac{1}{RR'}(2\dot{R}\dot{R}' - f') + \frac{1}{R^2}(\dot{R}^2 - f + K) = \kappa\tau^2\rho_{eff}. \quad (10)$$

Therefore (9) is also a valid solution of the Einstein field equations (A.12 - A.18 [4]) in this model. Making the assignment $R = r$ in (10) yields a more general version of (6), that is,

$$f' + \frac{f - K}{r} = -\kappa\tau^2\rho_{eff}r. \quad (11)$$

The solution of (11) is then

$$f(r) = -\frac{1}{3}\kappa\tau^2\rho_{eff}r^2 + \frac{8\pi G\rho_{eff}(0)}{c^2}\Delta^2, \quad (12)$$

where the constant $K = 8\pi G\rho_{eff}(0)\Delta^2/c^2$ determined from the last term of (8). Here ρ_{eff} is used and evaluated at $r = 0$.

In the above treatment we have initially assumed that the Universe has expanded over time and at any given epoch it has an averaged density ρ , which leads to ρ_{eff} . The solution of the field equations has been sought on this basis. However because the Carmeli metric is solved in an instant of time (on a cosmological scale) any time dependence is neglected. In fact, the general time dependent solution has not yet been found. But since we observe the expanding Universe with the coordinates of Hubble at each epoch (or redshift z) we see the Universe with a different density $\rho(z)$ and an effective density $\rho_{eff}(z)$. It is the form of this dependence on redshift z that is not accurately known, but in this paper, as in Paper I, I use a simple density model, which when used with Carmeli's equation (14) gives good agreement with observational supernovae data. Carmeli arrived at his solution with the

constant density assumption. I have made the implicit assumption that the solution is also valid if we allow the density to vary as a function of redshift, as is expected with expansion. See also [11].

The second term in (12) is a constant independent of r and describes a non-zero gravitational potential of a finite universe measured at the origin of coordinates. Note the sign of the second term compared to the first, which is a $-\rho_{eff}$ or negative density term.

But it follows from (4), (9) and (12) that

$$\frac{dr}{dv} = \tau \sqrt{1 + \left(\frac{1 - \Omega}{c^2 \tau^2} \right) r^2}, \quad (13)$$

where $\Omega = \rho/\rho_c$. This compares with the solution when the central potential is neglected (i.e. $\Delta \rightarrow 0$). In fact, the result is identical as we would expect in a universe where the Hubble law is universally true.

Therefore (13) may be integrated exactly and yields the same result as in Paper I,

$$\frac{r}{c\tau} = \frac{\sinh(\frac{v}{c}\sqrt{1 - \Omega})}{\sqrt{1 - \Omega}}. \quad (14)$$

Now the matter density as a function of redshift may be related by $\Omega = \Omega_m(1+z)^3$, where Ω_m is the averaged matter density, at the present epoch, expressed as a fraction of the critical or “closure” density. Here z , as in all of this paper, refers to the redshift resulting from the cosmological expansion of the Universe. Please see Paper I [12] for further discussion on the redshift dependence of Ω . As shown therein it is only necessary to modify the value of Ω_m to fit the form resulting from the influence of *spacevelocity* – or curvature – the result of the dependence described by (4).

It follows from (14) that

$$\frac{r}{c\tau} = \frac{\sinh(\beta\sqrt{1 - \Omega_m(1+z)^3})}{\sqrt{1 - \Omega_m(1+z)^3}}, \quad (15)$$

where

$$\beta = v/c = ((1+z)^2 - 1)/((1+z)^2 + 1), \quad (16)$$

the result of the relativistic Doppler effect. For v/c small $\beta \approx z$.

One of the goals of cosmology was to determine if the Hubble expansion is speed-limited. That is, that the photons we observe coming from the galaxies in the accelerating cosmic expansion are governed by the relativistic Doppler effect. This was answered in Paper I

where it was found that the speed-limited expansion with $\beta = ((1+z)^2 - 1)/((1+z)^2 + 1)$ is the only viable fit to the observational high- z SNe Ia data [12], predicted by Behar & Carmeli [1]. For this reason this form is also used here.

Regardless of the geometry of the Universe, provided it is spherically symmetric and isotropic on the large scale the description, (15) is identical to that we would get where the Universe has a unique center, with one difference which is explored in the following section. For an isotropic universe without a unique center, one can have an arbitrary number of centers. However if we are currently in a universe where the Galaxy is at the center of the local isotropy distribution this means the Universe we see must be very large and we are currently limited from seeing into an adjacent region with a different isotropy center.

III. GRAVITATIONAL POTENTIAL

In Paper I, the geometry in the model is the usual unbounded type, as found in an infinite universe, for example. In a finite bounded universe, one must consider an additional effect on the photons being received from the distant sources. The following equation describes the gravitational redshift (z_{grav}) resulting from the Galaxy sitting at the unique center of a finite spherically symmetric matter distribution. In this case we need to consider the difference in gravitation potential between the points of emission and reception of a photon. Hence we can write $g_{00} = 1 - 4\Phi/c^2$ where -4Φ is the gravitational potential, which is evaluated at r and the origin $r = 0$.

From the usual relativistic expression we get

$$\begin{aligned} 1 + z_{grav} &= \sqrt{\frac{g_{00}(0)}{g_{00}(r)}} \\ &= \frac{\sqrt{1 + 3(\Omega_m - 1) \left(\frac{\Delta}{c\tau}\right)^2}}{\sqrt{1 + (1 - \Omega) \left(\frac{r}{c\tau}\right)^2 + 3(\Omega_m - 1) \left(\frac{\Delta}{c\tau}\right)^2}} \end{aligned} \quad (17)$$

Equation (17) employs the time part of the 5D metric, which, up until this point, has not been considered in the metric describing the Hubble law universe. In an unbounded universe or where radius $\Delta \rightarrow \infty$, $1 + z_{grav} \rightarrow 1$. That is z_{grav} tends to zero.

In a finite bounded universe, the observed redshifts (z_{obs}) are actually related by

$$1 + z_{obs} = (1 + z_{grav})(1 + z), \quad (18)$$

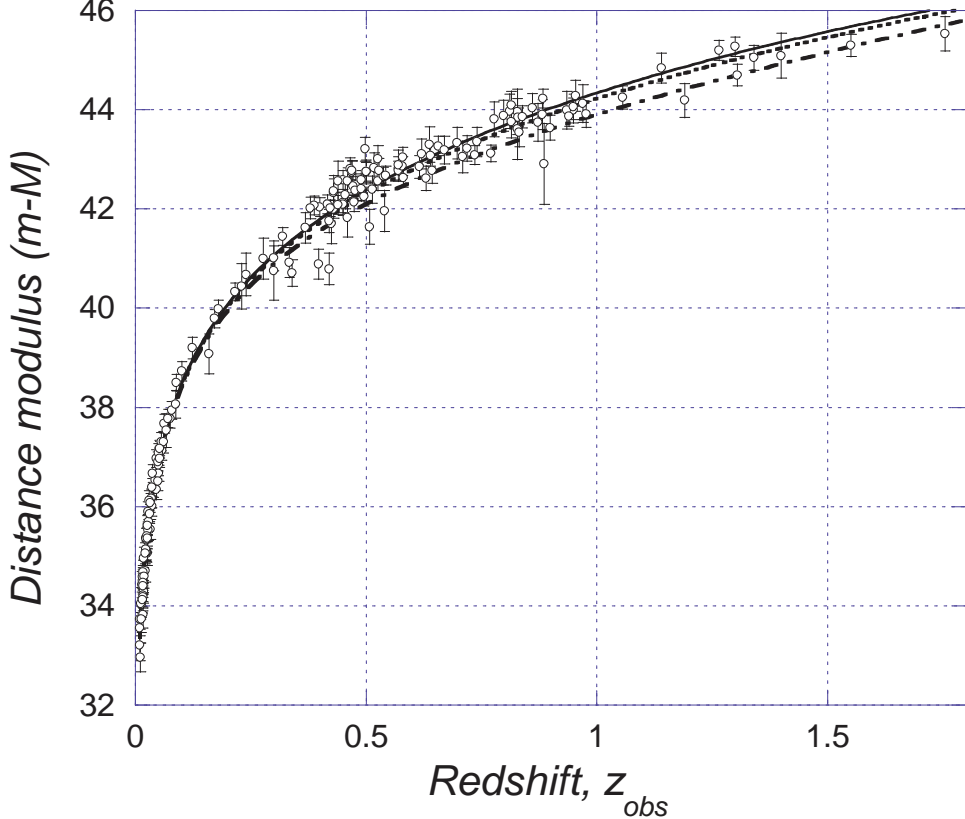


FIG. 1: Data taken from Table 5 of Riess *et al* [16]. All curves are fits with $\Omega_m = 0.021$ using the model described by (15). The solid line is the fit with $\Delta = 10^3 c\tau$, the dotted line is with $\Delta = 2 c\tau$ and the dot-dash line is with $\Delta = 1.2 c\tau$. Error bars are those taken from the published data

where z_{obs} represents the observed redshift and z is the cosmological redshift of the source as used in (15).

IV. HIGH-Z TYPE IA SUPERNOVAE

In order to compare (15) with the data from Riess *et al* [16] and Knop *et al* [13] the proper distance is converted to magnitude as follows.

$$m(z) - M_B = 5\log\left(\frac{c\tau}{Mpc}\right) + 25 + a + 5\log\mathcal{D}_L, \quad (19)$$

where \mathcal{D}_L is the dimensionless “Hubble constant free” luminosity distance. Refer [14, 15]. The units of $c\tau$ are Mpc . The constant 25 results from the luminosity distance expressed in Mpc . However, the first three terms in (19) represent a scale offset for the distance modulus ($m - M_B$), it is sufficient to include them in a single constant chosen from the fit. In practice,

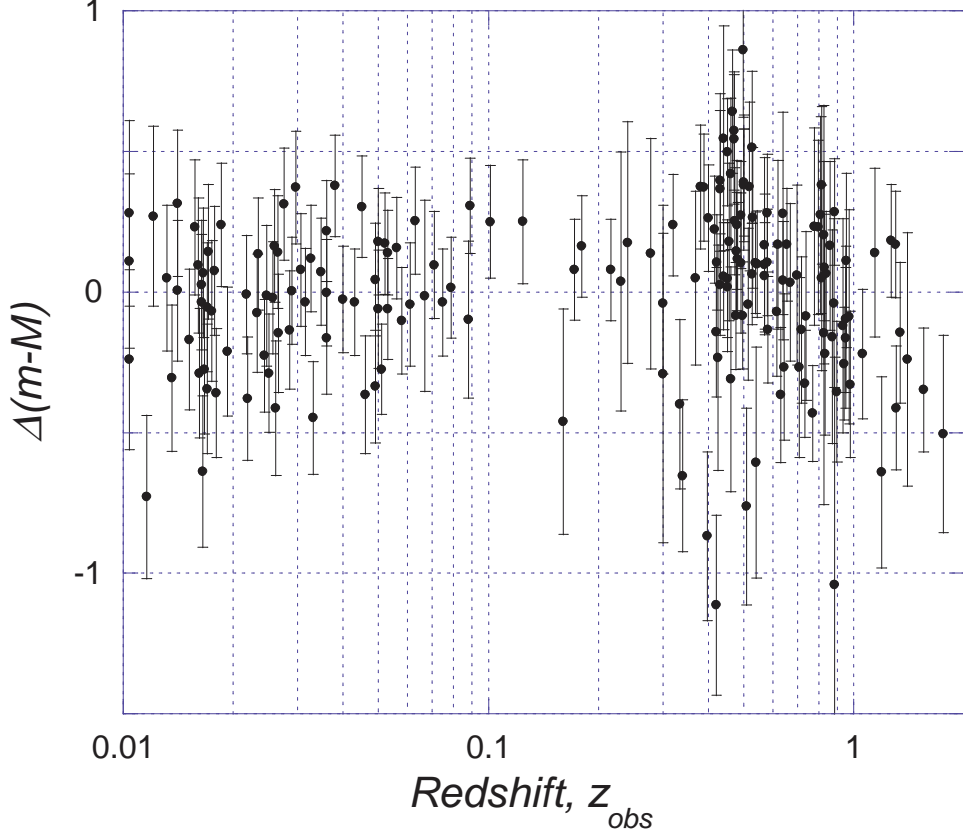


FIG. 2: Residuals: the differences between the curve with $\Delta = 3.6 c\tau$ and $a = 0.262$ and the data of Riess *et al* [16] shown fig. 1. The mean of the residuals is 0.00022 when all errors are assumed equal and 0.0324 when weighted by published errors with a standard error of 0.0167

a , a small free parameter is used to optimize the fits.

Because CGR is a theory based on the velocity dimension of the expanding universe, the distant sources are moving at high velocities (v) relative to the observer and it follows that the source masses undergo relativistic mass increase via the cosmological transformation,

$$M = M_0 \left(1 - \frac{t^2}{\tau^2}\right)^{-1/2} = M_0 (1 - \beta^2)^{-1/2}, \quad (20)$$

where M_0 is the source mass in its own rest frame. See [4, 6]. And since luminosity is proportional to mass (20) therefore leads to a luminosity increase according to

$$L = L_0 (1 - \beta^2)^{-1/2}, \quad (21)$$

where L_0 is the source luminosity in its own rest frame.

This then modifies the form of the luminosity distance by this factor and hence \mathcal{D}_L in

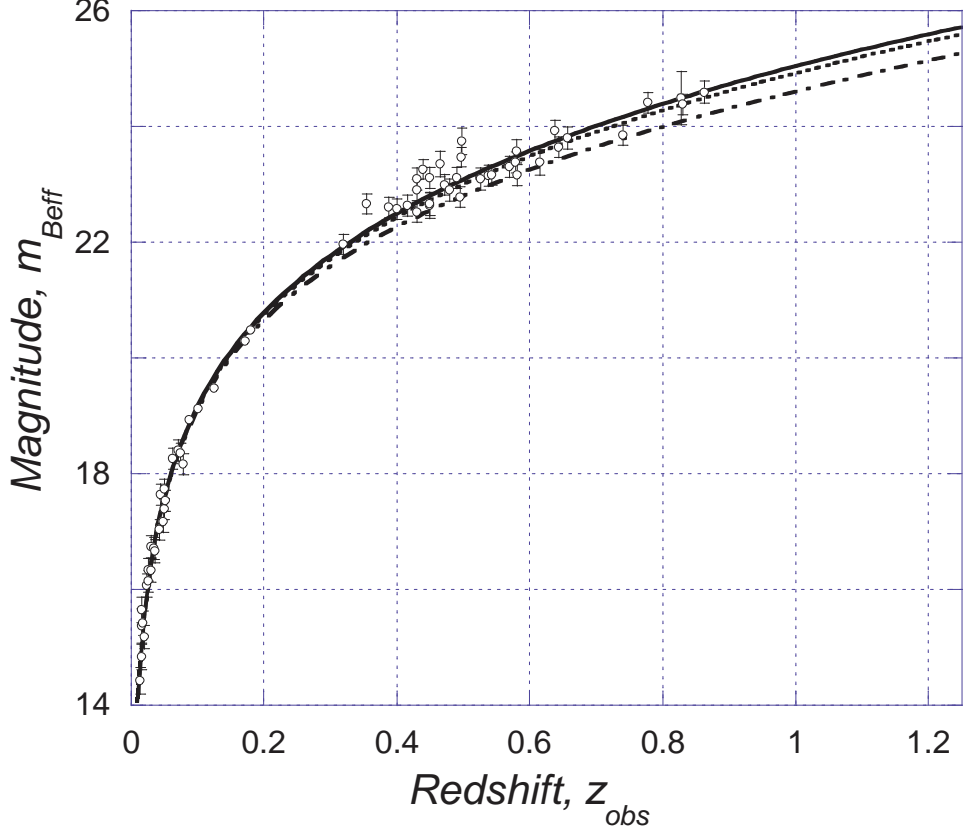


FIG. 3: These data are taken from column 4 of Tables 3 and 4 of Knop *et al* [13]. All curves are fits with $\Omega_m = 0.021$ using the model described by (15). The solid line is the fit with $\Delta = 10^3 c\tau$, the dotted line is with $\Delta = 2 c\tau$ and the dot-dash line is with $\Delta = 1.2 c\tau$. Error bars are those taken from the published data

CGR is given by

$$\mathcal{D}_L(z; \Omega_m, \Delta/c\tau) = \frac{r}{c\tau} (1 + z_{obs}) (1 - \beta^2)^{-1/2} \quad (22)$$

using (15) which is a function of Ω_m and z . And the cosmological redshift z in \mathcal{D}_L is related to the observed redshift z_{obs} by (17) and (18).

The parameter M_B in (19) is the absolute magnitude of the supernova at the peak of its light-curve, which acts as a “standard candle” from which the luminosity and hence distance can be estimated. In the case of (19) it is the distance modulus (denoted $m - M$) that is used. The details of the determination of M_B and the various corrections are left to the reader.

The value of the Hubble-Carmeli constant $\tau = h^{-1}$ cannot be uniquely determined from the fit. This is because the magnitude data are subject to an arbitrary offset. The zero

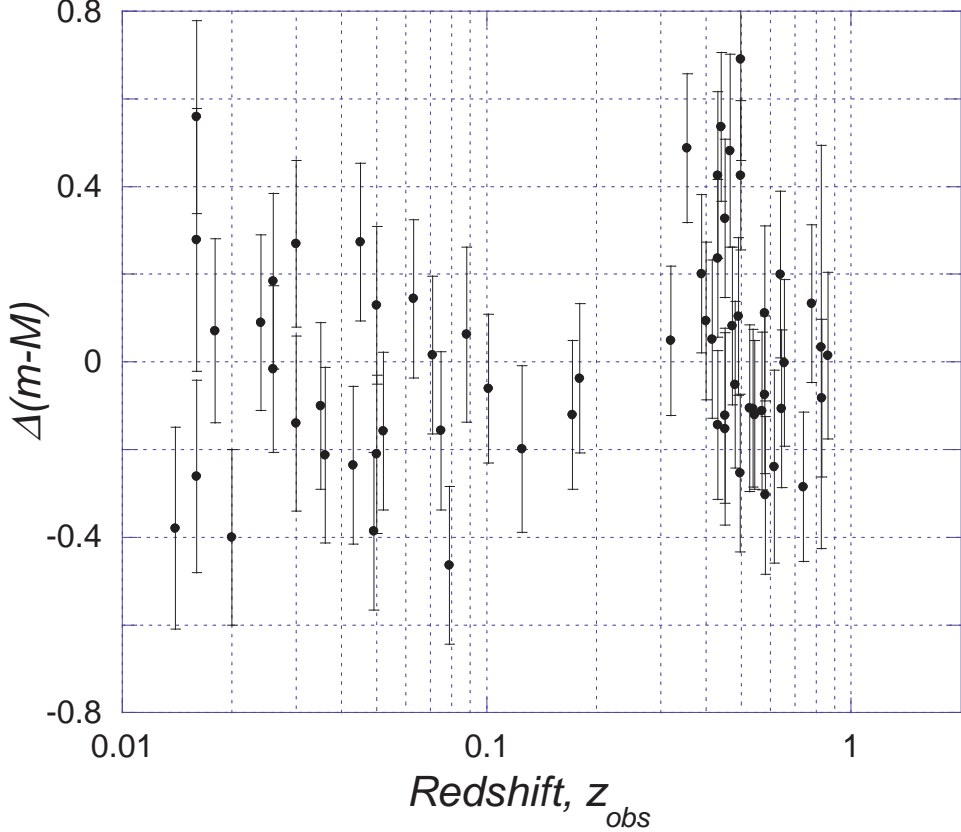


FIG. 4: Residuals: the differences between the curve with $\Delta = 3.6 c\tau$, $a = 0.262$ and $M_B = -19.3$ and the data of Knop *et al* [13] shown in fig. 3. The mean of the residuals is 0.0151 when all errors are assumed equal and 0.0105 when weighted by published errors with a standard error of 0.0237

point, the absolute magnitude of the fiducial SN Ia and the Hubble-Carmeli constant τ are all closely related and simply shift the data by an offset along the magnitude scale. Therefore in Riess *et al* [16] those quantities are arbitrarily set. However, in section V the value $h = 72.17 \pm 0.84$ km s⁻¹Mpc⁻¹ was determined from H_0 data as a function of distance. Using this value of h it follows that $5\log(c\tau/Mpc) + 25 = 43.0923$.

Equation (19) has been applied to the data from Table 5 of Riess *et al* [16] (shown in fig. 1) and Knop *et al* [13] (shown in fig. 3). The matter density $\Omega_m = 0.021$ was chosen from Paper I, for all fits because it is the average resulting from best fits to three different data sets. This paper compares models with this same value of normal baryonic matter density (no exotic dark matter) but different radii Δ .

Three curves are shown in figs 1 and 3. The solid line is the fit with $\Delta = 10^3 c\tau$, the dotted line with $\Delta = 2 c\tau$, and the dot-dash line is with $\Delta = 1.2 c\tau$. Allowing a and Δ

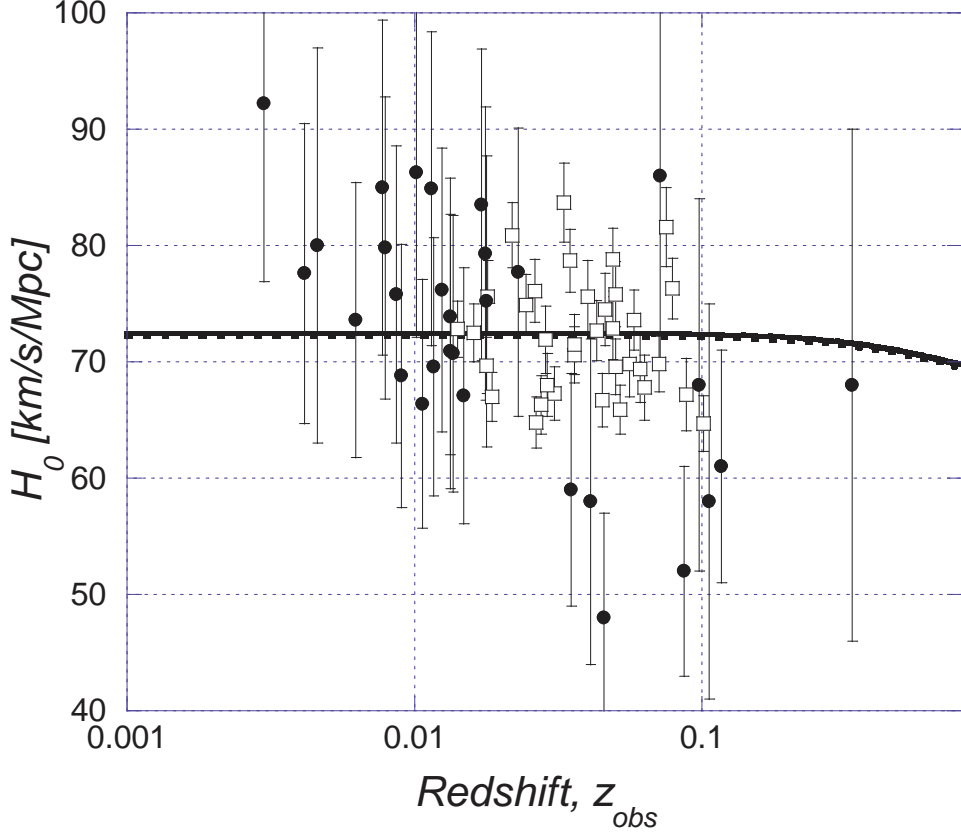


FIG. 5: Hubble constant H_0 as a function of redshift, z . The filled circles are determined from Tully-Fisher measurements taken from [7], Table 5 of [19] and Table 7 of [8], except the point at $z = 0.333$ is from Sunyaev-Zel'dovich effect taken from Fig. 4 of [19]. The open squares are determined from the SN Ia measurements and taken from Table 6 of [8] and Table 5 of [16]. The errors are those quoted in the sources from which the data was taken.

to run free over the whole data set the best fit curve resulted in $\Delta = (3.61 \pm 3.14) c\tau$ and $a = 0.262 \pm 0.036$. This curve is not shown in figs 1 and 3 because it would be difficult to resolve from the other curves, but it lays between the solid and dotted curves.

In order quantify the goodness of the least squares fitting the χ^2 parameter is used, which measures the goodness of the fit between the data and the theoretical curve assuming the two fit parameters a and Δ . Hence χ^2 is calculated from

$$\chi^2 = \sum_{i=1}^N \frac{1}{\sigma_i^2} [(m - M)(z)_i - (m - M)(z_{obs})_i]^2, \quad (23)$$

where N are the number of data; $(m - M)(z)$ are determined from (19) with fit values of a and Δ ; $(m - M)(z_{obs})$ are the observed distance modulus data at measured redshifts z_{obs} ;

σ_i are the published magnitude errors. The values of χ^2/N ($\approx \chi^2_{d.o.f.}$) are shown in Table I, calculated using published errors on the distance modulus data. In each case the best fit value of a is found for each value of Δ .

Table I: Curve fit parameters

Data set	N	$\Delta/c\tau$	a	χ^2/N
Riess <i>et al</i>	185	10^3	0.241	1.395
		3.6	0.262	1.388
		2.0	0.302	1.415
		1.2	0.441	1.809
Knop <i>et al</i>	63	10^3	0.260	1.677
		3.6	0.262	1.415
		2.0	0.313	1.769
		1.2	0.441	2.350

The χ^2/N values in Table I indicate a slight minimum when $\Delta = 3.6 c\tau$. Figs 2 and 4, respectively, show the residuals between the best fit curve with $\Delta = 3.6 c\tau$ and $a = 0.262$ and the Riess *et al* data from fig. 1 and Knop *et al* data from fig. 3. (An absolute magnitude $M_B = -19.3$ was added to the values of Knop *et al* data). In fig. 2 there may be a slight trend at high redshift $z_{obs} > 1$ which I suspect is the result of the density model not being accurate at high redshift.

Even so the best fit curve of figs 1 and 3 is only slightly different from the curve with $\Delta = 10^3 c\tau$. And the latter is negligibly different from curves with $\Delta = \infty$. In fact, they cannot be resolved on the same plot.

The data of fig. 1 are not determined better than the arbitrary scale offset. However Knop *et al* attempted to remove all uncertainties by making all possible corrections from which an effective magnitude ($m_{B_{eff}}$) was determined. See [13] for the details. Therefore their data contain the absolute magnitude of the fiducial SN Ia. An absolute magnitude of $M_B + a = -19.038$ was determined from the best fit assuming all other corrections have been taken into account in the data of fig. 3.

In both figs 1 and 3 curves for any value $\Delta \geq 2 c\tau$, are essentially equally good fits as

shown by the χ^2/N values in Table I. The differences in the fits are negligible on the scale of the errors in the modulus data. Nevertheless the fit with $\Delta = 3.6 c\tau$ is slightly favored. This means that the data are described by a universe with radius $\Delta \geq 2 c\tau$ and with a best fit for $\Delta = 3.6 c\tau$

In these analyzes only the flat *spacevelocity* model has been considered with the current epoch value $\Omega_m \approx 0.021$. In Paper I [12] a curved *spacevelocity* model was developed that took into account the gradient dr/dz which may be derived from (4). The analysis of the evolution of the matter density in the appendix of Paper I [12] is equally valid in this model. From that appendix the matter density in the curved *spacevelocity* model was found to only differ from the matter density in the flat *spacevelocity* model, up to a redshift $z = 2$, by a multiplying factor equal to approximately 1.28 and therefore the current epoch value $\Omega_m \approx 0.027$ in the curved *spacevelocity* model. However the correct density model is the subject of ongoing research.

Importantly, it is worth noting that the amount of matter necessary to achieve good fits to the data is within the bounds of measured baryonic matter [9]. Therefore this model does not require the existence of non-baryonic dark matter.

V. HUBBLE CONSTANT

Using the small redshift limit of (15) and the Hubble law at small redshift ($v = H_0 r$) it has been shown [4] that the Hubble parameter H_0 varies with redshift. If it applies at the low redshift limit it follows from the theory that at high redshift we can write

$$H_0 = h \frac{\beta \sqrt{1 - \Omega_m(1+z)^3}}{\sinh(\beta \sqrt{1 - \Omega_m(1+z)^3})}. \quad (24)$$

Therefore H_0 in this model is redshift dependent, not constant and $H_0 \leq h$. Only $h = \tau^{-1}$ is truly independent of redshift and constant. Therefore τ is a constant in the fits using (19). The condition where $H_0 = h$ only occurs at $z = 0$ or where $\Omega_m \rightarrow 0$.

By plotting H_0 values determined as a function of redshift, using (24), it is possible to get an independent determination of h , albeit the noise in the data is very large. This is shown in fig. 5 with values calculated by two methods with the exception of one point at $z = 0.333$. See figure caption for details. The data, even though very scattered, do indicate a trending down of H_0 with redshift.

Separate curve fits from (24), with h as a free parameter, have been applied to the two data sets, Tully-Fisher (TF) (the solid line) and SNe type Ia (the broken line) measurements. The former resulted in $h = 72.47 \pm 1.95$ (statistical) ± 13.24 (rms) $\text{km s}^{-1}\text{Mpc}^{-1}$ and from the latter $h = 72.17 \pm 0.84$ (statistical) ± 1.64 (rms) $\text{km s}^{-1}\text{Mpc}^{-1}$. The rms errors are they those derived from the published errors, the statistical errors are those due to the fit to the data alone. The SNe Ia determined value is more tightly constrained but falls within the TF determined value.

VI. DISCUSSION

In order to achieve a fit to the data, using either the finite bounded or unbounded models, the white hole solution of (6) or (11) must be chosen. The sign of the terms in (12), and hence also (17), means that the potential implicit in (12) is a potential hill, not a potential well. Therefore the solution describes an expanding white hole with the observer at the origin of the coordinates, the unique center of the Universe determined by Δ . Only philosophically can this solution be rejected, the data cannot distinguish a finite bounded model ($\infty > \Delta > c\tau$) from the infinite unbounded model ($\Delta = \infty$) using the Carmeli theory. However there is a indication from the fits that the Universe has a finite radius $\Delta = (3.61 \pm 3.14) c\tau$.

It is important to note also that in Carmeli's finite unbounded model ($\Delta = 0$) (15) describes the redshift distance relationship but no gravitational redshift effects are involved, because there is no central potential. In Paper I equation (15) was curved fitted to the same data that has been used here. Therefore the same conclusion applies.

The physical meaning is that the solution, developed in this paper, represents an expanding white hole centered on the Galaxy. The galaxies in the Universe are spherically symmetrically distributed around the Galaxy. The observed redshifts are the result of cosmological expansion and the gravitational potential hill centered on the Galaxy that the photons from distant sources must climb to reach the observer.

This is similar to the theoretical result obtained by Smoller and Temple [17] who constructed a new cosmology from the FRW metric but with a shock wave causing a time reversal white hole. In their model the total mass behind the shock decreases as the shock wave expands, which is spherically symmetrically centered on the Galaxy. Their paper states

in part "...the entropy condition implies that the shock wave must weaken to the point where it settles down to an Oppenheimer Snyder interface, (bounding a finite total mass), that eventually emerges from the white hole event horizon of an ambient Schwarzschild spacetime."

This result then implies that the earth or at least the Galaxy is in fact close to the physical center of the Universe. Smoller and Temple state [18] that "With a shock wave present, the *Copernican Principle is violated* in the sense that the earth then has a special position relative to the shock wave. But of course, in these shock wave refinements of the FRW metric, there is a spacetime on the other side of the shock wave, beyond the galaxies, and so the scale of uniformity of the FRW metric, the scale on which the density of the galaxies is uniform, is no longer the largest length scale" [emphasis added].

Their shock wave refinement of a critically expanding FRW metric leads to a big bang universe of finite total mass. This model presented here also has a finite total mass, is a spatially flat universe at the current epoch and the *spacetime* is approximately flat. It describes a finite bounded expanding white hole that started at some time in the past, though the time dependent solution has yet not been found, and has not been described here. The scale length of uniformity in this model is less than the largest length scale and therefore an effective radius is introduced.

VII. CONCLUSION

The Carmeli theory has been analyzed with distance modulus data derived by the high-z type Ia supernovae teams and found to be consistent with a universe that places the Galaxy at the center of an spherically symmetric isotropic expanding white hole of finite radius. The result describes particles moving in both a central potential and an accelerating expanding white hole universe without the need for the inclusion of dark matter. The radius of the finite matter distribution $\Delta \geq 2 c\tau$. The data cannot be used to exclude models with finite extensions.

The value of the Hubble constant in the limit of zero distance and zero gravity was also determined to be $h = 72.17 \pm 0.84 \text{ km s}^{-1}\text{Mpc}^{-1}$ from other independent type Ia SNe data.

Tully-Fisher distance data also yield a similar value using the Carmeli theory.

- [1] S. Behar, M. Carmeli, “Cosmological relativity: A new theory of cosmology”, *Int. J. Theor. Phys.* **39** (5): 1375-1396 (2000)
- [2] M. Carmeli, “Cosmological General Relativity”, *Commun. Theor. Phys.* **5**:159 (1996)
- [3] M. Carmeli, “Is galaxy dark matter a property of spacetime?”, *Int. J. Theor. Phys.* **37** (10): 2621-2625 (1998)
- [4] M. Carmeli, *Cosmological Special Relativity* (World Scientific, Singapore, 2002)
- [5] M. Carmeli, “Accelerating Universe: Theory versus Experiment”, [arXiv: astro-ph/0205396] (2002)
- [6] M. Carmeli, J.G. Hartnett, F.J. Oliveira, “The cosmic time in terms of the redshift,” arXiv:gr-qc/0506079, *Found. Phys. Letters* (in press) (2005)
- [7] W.L. Freedman, B.F. Madore, J.R. Mould, R. Hill, L. Ferrarese, R.C. Kennicutt Jr, A. Saha, P.B. Stetson, J.A. Graham, H. Ford, J.G. Hoessel, J. Huchra, S.M. Hughes and G.D. Illingworth, “Distance to the Virgo cluster galaxy M100 from Hubble Space Telescope observations of Cepheids”, *Nature* **371**: 757-762 (1994)
- [8] W.L. Freedman, B.F. Madore, B.K. Gibson, L. Ferrarese, D.D. Kelson, S. Sakai, J.R. Mould, R.C. Kennicutt Jr, H.C. Ford, J.A. Graham, J.P. Huchra, S.M.G. Hughes, G.D. Illingworth, L.M. Macri, and P.B. Stetson, “Final results from the Hubble Space Telescope Key Project to measure the Hubble constant”, *Ap. J.* **553**:47-72, (2001)
- [9] M. Fukugita, C.J. Hogan, and P.J.E. Peebles, “The cosmic baryon budget” *Ap. J.* **503**: 518-530 (1998)
- [10] W.W. Gibbs, “Profile: George F. R. Ellis”, *Scientific American* **273**(4): 28-29 (1995)
- [11] J.G. Hartnett, “Carmeli’s accelerating universe is spatially flat without dark matter”, *Int. J. Theor. Phys.* **44**(4): 485-492, (2005) [arXiv:gr-qc/0407083]
- [12] J.G. Hartnett, “The distance modulus determined from Carmeli’s cosmology fits the accelerating universe data of the high-redshift type Ia supernovae without dark matter,” *Found. Phys. Lett.* (in press) (2005) [arXiv:astro-ph/0501526]
- [13] R.A. Knop, G. Aldering, R. Amanullah, P. Astier, G. Blanc, M. S. Burns, A. Conley, S. E. Deustua, M. Doi, R. Ellis, S. Fabbro, G. Folatelli, A. S. Fruchter, G. Garavini, S. Garmond,

K. Garton, R. Gibbons, G. Goldhaber, A. Goobar, D. E. Groom, D. Hardin, I. Hook, D. A. Howell, A. G. Kim, B. C. Lee, C. Lidman, J. Mendez, S. Nobili, P. E. Nugent, R. Pain, N. Panagia, C. R. Pennypacker, S. Perlmutter, R. Quimby, J. Raux, N. Regnault, P. Ruiz-Lapuente, G. Sainton, B. Schaefer, K. Schahmaneche, E. Smith, A. L. Spadafora, V. Stanishev, M. Sullivan, N. A. Walton, L. Wang, W. M. Wood-Vasey, and N. Yasuda, “New constraints on Ω_M , Ω_Λ and w from an independent set of 11 high-redshift supernovae observed with the Hubble Space Telescope”, *Ap. J.* **598**: 102-137 (2003)

[14] S. Perlmutter, S. Gabi, G. Goldhaber, A. Goobar, D.E. Groom, I.M. Hook, A.G. Kim, M.Y. Kim, J.C. Lee, R. Pain, C.R. Pennypacker, I.A. Small, R.S. Ellis, R.G. McMahon, B.J. Boyle, P.S. Bunclark, D. Carter, M.J. Irwin, K. Glazebrook, H.J.M. Newberg, A.V. Filippenko, T. Matheson, M. Dopita, and W.J. Couch, “Measurements of the cosmological parameters Ω and Λ from the first seven supernovae at $z > 0.35$ ”, *Ap. J.* **483**:565-581 (1997)

[15] A.G. Riess, A. V. Filippenko, P. Challis, A. Clocchiatti, A. Diercks, “Observational evidence from supernovae for an accelerating universe and a cosmological constant”, *Astron. J.* **116**: 1009-1038 (1998)

[16] A.G. Riess, L-G Strolger, J. Tonry, S. Casertano, H. C. Ferguson, B. Mobasher, P. Challis, A.V. Filippenko, S. Jha, W. Li, R. Chornock, R.P. Kirshner, B. Leibundgut, M. Dickinson, M. Livio, M. Giavalisco, C.C. Steidel, T. Benítez and Z. Tsvetanov, “Type Ia supernovae discoveries at $z > 1$ from the Hubble Space Telescope: Evidence for past deceleration and constraints on dark energy evolution” *Ap. J.* **607**: 665-687 (2004)

[17] J. Smoller and B. Temple, PNAS **100**(20): 1121611218 (2003)

[18] J. Smoller and B. Temple, <http://www.math.ucdavis.edu/~temple/articles/temple1234.pdf>

[19] Y. Tutui *et al.* (2001). PASJ. **53**: 701. [arXiv:astro-ph/0108462]